Real-Time Joint Estimation of Queue Dynamics and Arrival Time via a Car-Following-Model-Integrated Unscented Kalman Filter

Qiongdan Hu*[1], Chaopeng Tan[1], Menglin Yang[1], and Meng Wang[1]

[1]Chair of Traffic Process Automation, Technische Universität Dresden, Dresden 01069, Germany

Short summary

Optimizing trajectories of Connected and Automated Vehicles (CAVs) and signal plans requires precise real-time prediction of the Time of Arrival (ToA) at signalized intersections. Although CAVs feature advanced sensors that capture high-fidelity microscopic dynamics, their limited spatial coverage restricts the continuous observation of macroscopic queue profiles. To overcome this limitation, this paper proposes a real-time data fusion method integrating these mobile sensor data with a conventional stopline loop detector to jointly estimate queue length and predict ToA in mixed traffic environments. Specifically, the proposed method first initializes a macroscopic queue state using historical arrival patterns and data from stop line sensors. Subsequently, as the leader of the CAV decelerates, an Intelligent Driver Model-integrated Unscented Kalman Filter is triggered to continuously fuse the data of high-fidelity onboard sensors and shockwave dynamics. Under oversaturated conditions, the proposed method improves ToA prediction by reducing errors by 20.2% and 8.6% against pure macroscopic and moving-average constant deceleration baselines, respectively. By resolving the scale gap between macroscopic queue dynamics and microscopic car-following dynamics, this framework provides reliable predictions of queue length and ToA of CAVs.

Keywords: Connected and Automated Vehicles; Traffic State Estimation; Kalman Filter; Mobile Sensing; Traffic Flow Theory

1 Introduction

Real-time estimation of queue length and time of arrival (ToA) for public transport (PT) is essential for adaptive traffic signal control (Hu et al., 2022). Traditional fixed-location sensors capture macroscopic traffic states but cannot continuously track dynamic, backward-propagating queue tails, lacking the real-time data needed to accurately predict ToA (Viti & Van Zuylen, 2010; Ramezani & Geroliminis, 2015). Concurrently, autonomous PT vehicles equipped with advanced onboard sensors provide high-fidelity, real-time microscopic measurements (Feng et al., 2019). However, their localized sensing range and low penetration rate yield highly sparse spatial observations, preventing independent queue state reconstruction (Makridis & Kouvelas, 2023). Bridging this observability gap requires integrating the microscopic sensing of autonomous PT vehicles with macroscopic data from fixed detectors for joint queue and ToA estimation.

Both queue estimation and ToA prediction have been extensively studied, yet integrating them in real-time under sparse observability remains unresolved. For queue estimation, macroscopic kinematic wave models effectively capture shockwave boundaries using fixed-sensor data (Lighthill & Whitham, 1955). However, fixed detectors at the stop line fail to capture stochastic traffic dynamics upstream, yielding macroscopic boundaries that cannot resolve precise vehicle-level queue tails. Conversely, microscopic car-following models simulate precise vehicle movements but demand continuous trajectory inputs. Without high-frequency sensor updates, unobserved driver variations rapidly accumulate, causing divergence between simulated and actual trajectories (Treiber & Kanagaraj, 2015). Furthermore, while data-driven methods demonstrate high accuracy, they fundamentally demand massive historical training data, restricting their transferability to instantaneous signal control under sparse observations.

Predicting the exact ToA for approaching vehicles is critical for signal optimization. Existing ToA prediction methods rely on either analytical models based on aggregated macroscopic parameters,

or data-driven frameworks that lack explicit physical formulations to capture sudden traffic perturbations. Crucially, both approaches fail to explicitly model the high-fidelity dynamic interception process—the continuous spatiotemporal convergence between an approaching vehicle's stochastic trajectory and the highly dynamic, backward-propagating microscopic queue tail. This disconnect between macroscopic assumptions and continuous microscopic dynamics introduces systemic errors, directly degrading the reliability of real-time transit signal priority.

To address these challenges—and specifically to explore the feasibility of joint estimation in extremely sparse scenarios, such as relying on a single approaching CAV. This study proposes a real-time, Intelligent Driver Model (IDM)-integrated data fusion framework. As illustrated in Figure 1, the blue vehicle represents a CAV equipped with onboard ranging sensors to measure the real-time spacing and speed of its immediate leader. Meanwhile, macroscopic traffic counts from the fixed stop-line loop detector are used to initialize the system state. The proposed method fuses these two data sources to continuously estimate the dynamic queue length and predict the ToA.

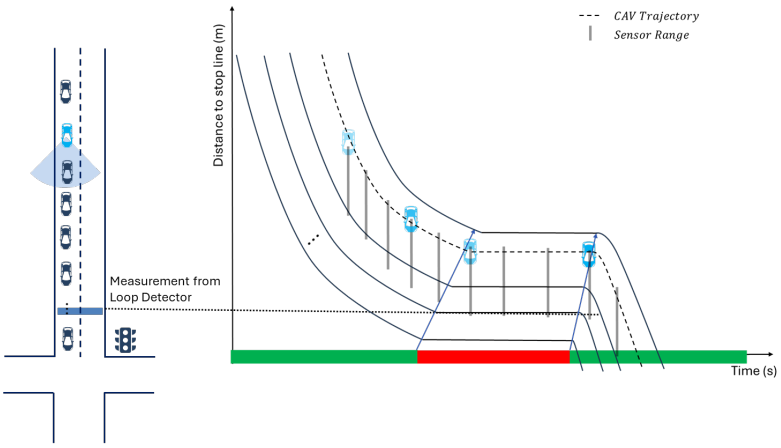


Figure 1: Time-space diagram of a sensor-equipped CAV approaching a signalized intersection

The proposed method is built upon three fundamental assumptions: (1) First-In-First-Out discipline, where lane-changing is ignored to preserve invariant longitudinal ordering; (2) deterministic discharge rates and signal timings are provided by stop-line loop detectors and Vehicle-to-Infrastructure (V2I) communication, respectively; and (3) the CAV captures the real-time trajectory of itself and its immediate preceding vehicle via onboard sensors.

The methodology is sequentially structured into Initialization, Estimation, and Prediction modules, as illustrated in Figure 2. Initially, the shockwave model processes loop detector data to establish a macroscopic initial condition of the queue boundary. Subsequently, the Estimation phase is triggered when the CAV's immediate leader decelerates to join the queue. Taking the macroscopic boundary as the initial state, an IDM-integrated Unscented Kalman Filter (UKF) recursively fuses the IDM-predicted leader behavior with the CAV's onboard sensor measurements. By optimally weighing the macroscopic physical constraints and real-time microscopic observations

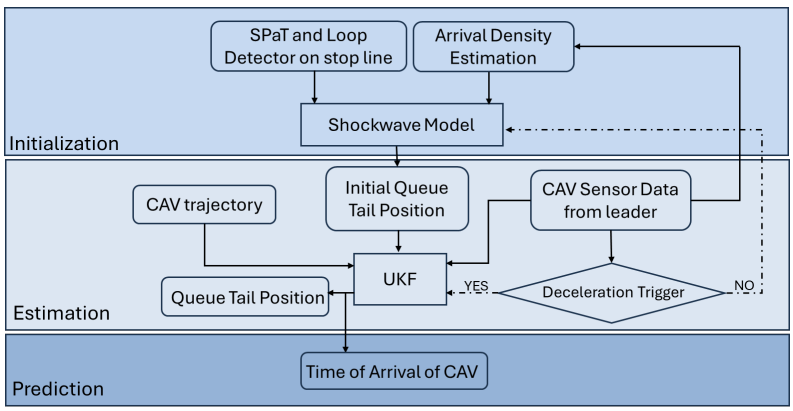


Figure 2: IDM-Integrated UKF Framework

based on their error covariance matrices, the UKF corrects macroscopic cumulative drifts and continuously tracks the real-time microscopic queue tail. Finally, the Prediction module utilizes these continuously updated states to formulate a dynamic integral equation. This calculates the exact interception time between the CAV and the backward-propagating shockwave, ultimately outputting the predicted ToA and the expected queue tail position at the time of arrival. We validate the proposed framework through SUMO simulations under oversaturated conditions, bench-marking its predictive performance against pure macroscopic shockwave baseline and naive kinematic baselines.

2 Macroscopic Queue Tail Initialization

The upstream traffic state is initialized using the historical average arrival flow q_{in} . Assuming traffic flow conservation, q_{in} is approximated by the long-term average throughput measured at the stop-line loop detector. According to the triangular fundamental diagram, the corresponding arrival density is defined as $\rho_{in} = q_{in}/v_f$, where the free-flow speed v_f is a predetermined physical parameter that can be calibrated using the road's speed limit or the CAV's initial cruising speed. The positions of the macroscopic queue tail $p^{mac}_{tail}(k)$ and head $p^{mac}_{head}(k)$ evolve according to the shockwave speeds w_{tail} and $w_{head}(k)$:

$$w_{tail} = \frac{-q_{in}}{\rho_{jam} - \rho_{in}}, \quad w_{head}(k) = \frac{-q_{out}(k)}{\rho_{jam} - \rho_{out}(k)} \tag{1}$$

where ρ_{jam} is the jam density, $q_{out}(k)$ is the discharge flow, and $\rho_{out}(k)$ is the discharge density. Given the distance-to-stop-line coordinate p, the queue tail and head positions are updated as:

$$p^{mac}_{tail/head}(k+1) = p^{mac}_{tail/head}(k) + w_{tail/head}(k)\Delta t \tag{2}$$

During red intervals where $q_{out} = 0$, the queue head remains stationary at the stop line, i.e., $p^{mac}_{head} = 0$. Conversely, green phases trigger upstream dissipation at a constant absolute speed of $|w_{head}|$.

3 High-Fidelity Queue Tail Estimation via UKF

To resolve macroscopic estimation errors, the UKF is applied. When the CAV approaches the queue, its preceding vehicle L decelerates, triggering the UKF to continuously track the high-fidelity queue tail (Wu et al., 2005).

State Vector and System Dynamics

The UKF state vector $\mathbf{x}_k$ continuously tracks the leader's kinematics and the evolving queue tail simultaneously:

$$\mathbf{x}_k = [p_L(k), v_L(k), p^{mic}_{tail}(k), w^{mic}(k)]^T \tag{3}$$

Here w^{mic} is the microscopic shockwave speed. At the triggering moment k_0 , the framework initializes the state vector by bridging the domains: the queue tail position and shockwave speed are inherited from macroscopic estimates ($p^{mic}_{tail}(k_0) = p^{mac}_{tail}(k_0)$ and $w^{mic}(k_0) = w_{tail}$), while the leader's kinematics ($p_L(k_0)$ and $v_L(k_0)$) are extracted from the CAV's onboard sensors. The IDM (Treiber & Kanagaraj, 2015) predicts the leader's deceleration based on the relative closing rate to the queue tail position. Given the distance-to-stop-line coordinate, the expected acceleration $a_L(k)$ is computed as:

$$a_L(k) = a\left[1 - \left(\frac{v_L(k)}{v_0}\right)^4 - \left(\frac{s_0 + \max\left(0, v_L(k)T + \frac{v_L(k)\Delta v(k)}{2\sqrt{ab}}\right)}{p_L(k) - p^{mic}_{tail}(k)}\right)^2\right] \tag{4}$$

where $\Delta v(k) = v_L(k) - w^{mic}(k)$ is the approaching rate between the forward-moving vehicle and the backward-propagating tail. The state transition is formulated as:

$$\mathbf{x}_{k+1} = \begin{bmatrix} p_L(k) - v_L(k)\Delta t - \frac{1}{2}a_L(k)\Delta t^2 \\ \max(v_L(k) + a_L(k)\Delta t, 0) \\ p^{mic}_{tail}(k) + w^{mic}(k)\Delta t \\ w^{mic}(k) \end{bmatrix} + \boldsymbol{\xi}_k \tag{5}$$

where $\boldsymbol{\xi}_k \sim N(\mathbf{0}, \mathbf{Q}_{mic})$ represents the process noise vector. The covariance matrix $\mathbf{Q}_{mic}$ accounts for the modeling uncertainties in individual car-following behavior and dynamic fluctuations in the microscopic shockwave speed.

Measurement Update and Dynamic Confidence

The CAV's onboard sensor provides linear measurements of the leader's kinematics: $\mathbf{z}_k = \mathbf{H}\mathbf{x}_k + \boldsymbol{\eta}_{mic}(k)$, where $\mathbf{z}_k = [p_L^{sensor}(k), v_L^{sensor}(k)]^T$ and the observation matrix is $\mathbf{H} = [\mathbf{I}_{2\times2}\ \mathbf{0}_{2\times2}]$. The UKF computes the Kalman Gain to optimally weigh sensor measurements against IDM-based state predictions. Note that the variance of the estimated queue tail $\sigma_{tail}^2(k)$, corresponding to the $(3,3)$ element of the error covariance matrix $\mathbf{P}_k$, serves as the confidence indicator. As the leader vehicle reaches a complete standstill, the physical tail position becomes deterministic, causing $\sigma_{tail}^2(k)$ to decrease, reflecting higher estimation certainty.

4 Expected Time of Arrival Prediction

Once the UKF is tracking the queue tail, the cumulative drift inherent in the macroscopic estimation is dynamically mitigated. Assuming uniform linear motion produces significant ToA errors against dynamic, backward-propagating shockwaves. To avoid this, the framework integrates the future trajectories of the CAV and the shockwave to define two critical variables: the free-flow intercept time T_{free} (the duration required for the CAV to catch the queue tail) and the interception coordinate p_{int} (the exact spatial location of convergence). As illustrated in Figure 3, projecting the CAV's trajectory against the estimated shockwaves naturally decomposes the arrival process into this free-flow interception phase and a subsequent queue discharge phase (T_{queue}).

$$p_{\text{CAV}}(t_k) - v_f \cdot T_{free} = p_{tail}^{mic}(t_k) + w^{mic}(t_k) \cdot T_{free} = p_{int} \tag{6}$$

This equation transitions the discrete-time tracking into a predictive formulation, where t_k denotes the continuous time corresponding to the current estimation step k. Here, $p_{tail}^{mic}(t_k)$ and $w^{mic}(t_k)$ designate the precise tail position and microscopic shockwave speed estimated by the IDM-integrated UKF. The term v_f serves as the CAV's anticipated approach velocity. The queuing

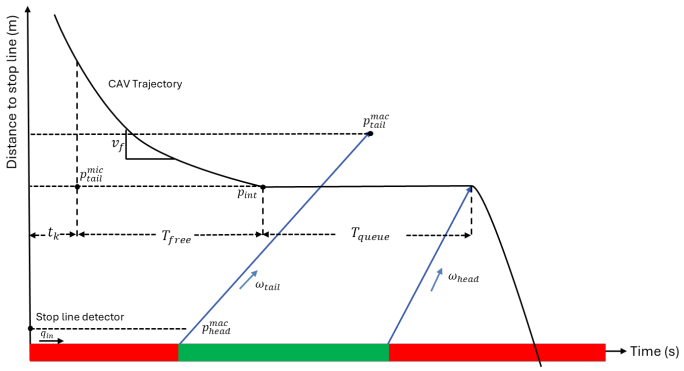


Figure 3: Time-space diagram of the ToA prediction based on IDM-UKF

delay T_{queue} incorporates signal timings via a green phase indicator $I_{green}(\tau) \in \{0, 1\}$. It represents the time required to accumulate sufficient effective green capacity to discharge all queued vehicles located between the interception point p_{int} and the stop line. In multi-cycle and oversaturated scenarios, the spatial accumulation of waiting vehicles is quantified by the jam density ρ_{jam} multiplied by the interception distance p_{int}. The queueing delay is therefore calculated by solving:

$$\int_{t_k+T_{free}}^{t_k+T_{free}+T_{queue}} q_{out} \cdot I_{green}(\tau)\, d\tau = p_{int} \cdot \rho_{jam} \tag{7}$$

This formulation integrates over the continuous chronological signal sequence to account for residual queues caused by oversaturation. When the accumulated queued vehicles $p_{int} \cdot \rho_{jam}$ exceed the discharge capacity of a single cycle, the integral naturally extends across subsequent red intervals characterized by $I_{green}(\tau) = 0$ and into successive cycles until the total required discharge capacity is satisfied. The predicted arrival time at the stop line is determined by $\text{ToA} = t_k + T_{free} + T_{queue}$.

5 Results and discussion

Experimental Setup

To replicate multi-cycle oversaturation, a two-stage departure logic is implemented: an initial dense platoon establishes a residual queue during a 60-second red phase, followed by a sparse fleet representing free-flow approaching traffic. Ground truth queue membership is determined by a speed threshold below 2.0 m/s within 250 m of the stop line, utilizing a 7.5 m jam spacing and a 1.0 s simulation time step. A total of 20 vehicles are deployed, yielding 19 evaluated CAV scenarios. The departure scheme is structured to generate two distinct traffic regimes: 10 vehicles approach under under-saturated conditions, 9 vehicles encounter oversaturated conditions. Ground truth queue is determined by a speed threshold of 2.0 m/s within 250 m of the stop line.
To replicate onboard sensor perception, measurement noise is added to the simulated trajectories. Position measurements include distance-dependent Gaussian noise with a standard deviation of $\sigma_p = 0.5 + 0.02 \cdot \Delta x$ meters, where Δx is the spacing to the preceding vehicle. Speed measurements include a constant noise with a standard deviation of $\sigma_v = 0.2$ m/s. The UKF utilizes standard scaled Unscented Transform parameters ($\alpha = 0.3$, $\beta = 2$, $\kappa = 0$) and implemented using the dynamic state estimation method proposed by Qi et al. (2018). To ensure physical validity, tracking activates only when the leader decelerates for consecutive steps.

Performance and Analysis

The performance evaluation begins by verifying the spatiotemporal queue dynamics against the ground truth. Figure 4 presents the queue tail estimation for Vehicle 16 under an oversaturated regime. Prior to UKF activation, the macroscopic and naive (3-step moving-average speed with constant-deceleration stopping estimate) baselines provide only a rough approximation of the ground truth queue tail (< 2.0 m/s), failing to capture fine-grained shockwave dynamics. The UKF tracking triggers upon detecting sustained leader deceleration ($< -0.5\,\mathrm{m/s^2}$). Once active, the UKF posterior mean rapidly converges to the ground truth. Concurrently, the 3σ confidence band narrows progressively as kinematic measurements are assimilated, demonstrating robust online queue tail estimation under oversaturated queue.

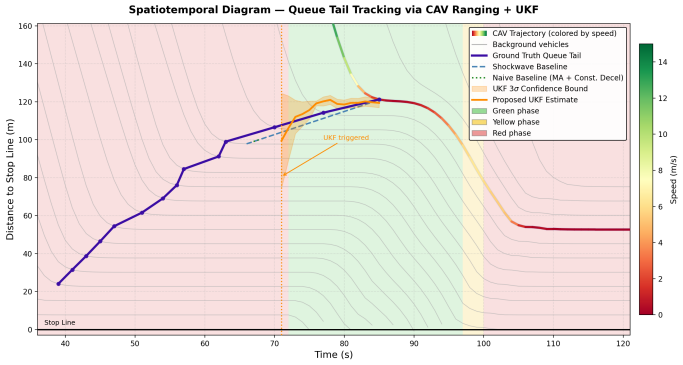
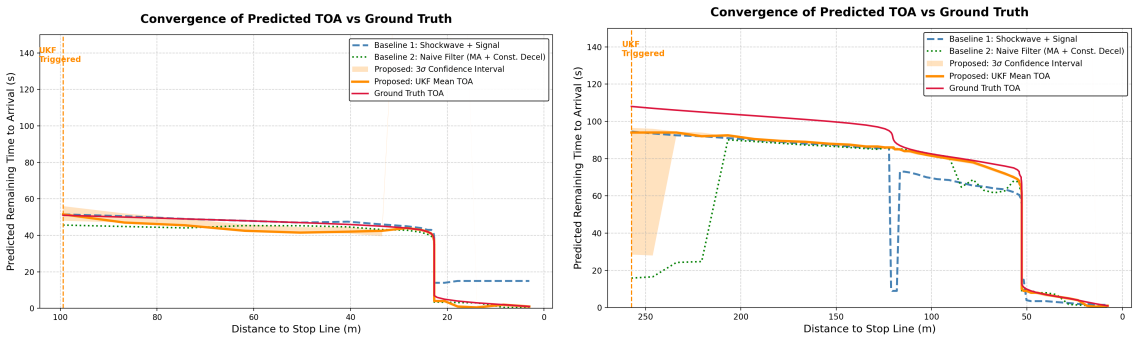


Figure 4: Spatiotemporal evolution of the queue tail of CAV 16 over time.

Building upon this queue tail estimation, ToA prediction accuracy is evaluated as the CAV progresses toward the stop line. Figure 5 presents the qualitative convergence of ToA predictions under two representative traffic scenarios, while Table 1 quantifies the prediction errors across all 19 simulation runs. All predictions are evaluated from the UKF activation frame onward to ensure identical temporal windows.
Figure 5a illustrates the ToA convergence for Vehicle 3, serving as the most typical and representative case for the under-saturated scenario ($N = 10$) evaluated in Table 1. The queue dissipates within a single green phase, rendering signal delay relatively unambiguous. Consequently, both baselines approximate the ground truth reasonably well. As reflected by the group averages in Table 1, the proposed UKF yields a ToA Mean Absolute Error(MAE) of 4.15 s across all under-saturated cases, providing only marginal improvements over the Naive Filter under such single-cycle conditions.
Conversely, Figure 5b demonstrates the ToA prediction evolution under an oversaturated condition. The naive baseline captures instantaneous speed changes but lacks global awareness of downstream



(a) ToA prediction under single-cycle queueing scenario (Vehicle 3)

(b) ToA prediction under oversaturated queueing scenario (Vehicle 16)

Figure 5: Convergence predicted ToA of veh 3 and veh 16

macroscopic queue evolution, resulting in delayed responses to residual queues. The shockwave baseline exhibits a distinct phase-boundary overdrift at approximately 100 m: a single-frame signal transition causes the estimated queuing delay to collapse, exposing its vulnerability in oversaturated conditions. The IDM-integrated UKF, fusing real-time kinematic measurements with shockwave constraints, identifies that the residual queue extends beyond the initial green phase, maintaining a smooth, monotonically converging ToA estimate. Quantitatively, the UKF reduces ToA MAE in oversaturated conditions to 25.38 s, outperforming the Naive Filter (27.87 s) and Shockwave model (29.71 s).

Table 1: Performance Evaluation of ToA Prediction and Queue Tail Estimation

Metrics & Scenarios	**Prediction Models**		
	Shockwave	Naive Filter	Proposed UKF
MAE of Predicted ToA (s)			
Under-Saturated (N=10)	7.08	4.45	4.15
Oversaturated (N=9)	29.71	27.87	25.38
Average (N=19)	17.80	15.54	14.21
MAE of Queue Tail (vehicles)			
Under-Saturated (N=10)	3.49	0.80	1.54
Oversaturated (N=9)	4.33	1.19	1.73
Average (N=19)	3.89	0.98	1.63

Table 1 summarises predictive accuracy across all 19 simulation runs. To ensure statistical robustness, each vehicle is sequentially designated as the CAV, and MAE is computed from the UKF activation frame to the stop-line crossing. Averaged across all 19 runs, the proposed method reduces ToA MAE by 20.2% relative to baseline 1 Shockwave and 8.6% relative to baseline 2 Naive Filter. The gains are substantially larger under oversaturated conditions (two or more experienced red phases), where the proposed method outperforms baseline 2 in 14 of 19 scenarios. Additionally, in terms of queue tail estimation, the macroscopic shockwave method exhibits larger errors, whereas the two filtering approaches demonstrate comparable performance. These results confirm that while constant-rate assumptions suffice for simple, under-saturated queues, IDM-integrated online prediction is indispensable for reliable ToA prediction under oversaturated queueing scenarios and high-demand environments.

6 Conclusions

This study proposes a real-time, IDM-integrated UKF framework to jointly estimate dynamic queue tails and predict ToA for CAVs at signalized intersections. By integrating macroscopic kinematic wave theory with CAV onboard measurements, the method mitigates cumulative drift and accounts for multi-cycle residual queues. Simulation results across 19 scenarios show that the proposed method outperformed macroscopic and naive filter baselines in 89% and 74% of cases, respectively. Overall, it reduced ToA MAE by 20.2% and 8.6% compared to these baselines. Under

oversaturated conditions, the ToA prediction error was reduced to 25.38 seconds, representing a 14.6% and 8.9% improvement over the macroscopic and naive baselines. While the naive filter yields slightly lower spatial queue estimation errors, the proposed framework provides superior temporal forecasting across cycles. These improved ToA predictions can directly support advanced intersection signal control and CAV trajectory optimization.

Acknowledgements

This research is part of the AgiMo project, funded by the Deutsche Forschungsgemeinschaft (DFG, German Research Foundation) - TRR: 408/1 2025 - Project number: 531327426.

Statement

Google Gemini was utilized for language refinement during the writing process. The authors reviewed the output and assume full responsibility for the final content.

References

Feng, D., Rosenbaum, L., Timm, F., & Dietmayer, K. (2019). Leveraging Heteroscedastic Aleatoric Uncertainties for Robust Real-Time LiDAR 3D Object Detection. In *2019 IEEE Intelligent Vehicles Symposium (IV)* (pp. 1280–1287). (ISSN: 2642-7214)

Hu, S., Zhou, Q., Li, J., Wang, Y., Roncoli, C., Zhang, L., & Lehe, L. (2022). High Time-Resolution Queue Profile Estimation at Signalized Intersections Based on Extended Kalman Filtering. *IEEE Transactions on Intelligent Transportation Systems*, *23*(11), 21274–21290. (GSCC: 0000027 2026-01-26T18:22:11.846Z 0)

Lighthill, M. J., & Whitham, G. B. (1955). On kinematic waves II. A theory of traffic flow on long crowded roads. *Proceedings of the Royal Society of London. A. Mathematical and Physical Sciences*, *229*(1178), 317–345.

Makridis, M. A., & Kouvelas, A. (2023). An adaptive framework for real-time freeway traffic estimation in the presence of CAVs. *Transportation Research Part C: Emerging Technologies*, *149*, 104066.

Qi, J., Sun, K., Wang, J., & Liu, H. (2018). Dynamic State Estimation for Multi-Machine Power System by Unscented Kalman Filter With Enhanced Numerical Stability. *IEEE Transactions on Smart Grid*, *9*(2), 1184–1196.

Ramezani, M., & Geroliminis, N. (2015). Queue Profile Estimation in Congested Urban Networks with Probe Data. *Computer-Aided Civil and Infrastructure Engineering*, *30*(6), 414–432. (GSCC: 0000206 2025-11-07T15:59:57.868Z 0)

Treiber, M., & Kanagaraj, V. (2015). Comparing numerical integration schemes for time-continuous car-following models. *Physica A: Statistical Mechanics and its Applications*, *419*, 183–195.

Viti, F., & Van Zuylen, H. J. (2010). Probabilistic models for queues at fixed control signals. *Transportation Research Part B: Methodological*, *44*(1), 120–135. (GSCC: 0000104 2025-12-05T09:51:47.935Z 0)

Wu, Y., Hu, D., Wu, M., & Hu, X. (2005). Unscented Kalman filtering for additive noise case: augmented vs. non-augmented. In *Proceedings of the 2005, American Control Conference, 2005.* (pp. 4051–4055 vol. 6). (ISSN: 2378-5861)